PROCEEDINGS OF SCIENCE

Refined Estimates of Carbon Abundances for Carbon-Enhanced Stars

Silvia Rossi[1], **Vinicius M. Placco**
Departament of Astronomy, IAG
Universidade de São Paulo, Rua do Matão 1226, Brazil
E-mail: rossi@astro.iag.usp.br, vmplacco@astro.iag.usp.br

Timothy C. Beers, Catherine R. Kennedy, Brian Marsteller
Dept. of Physics & Astronomy and JINA: Joint Institute for Nuclear Astrophysics,
Michigan State University, E. Lansing, MI 48824 USA
E-mail: beers@pa.msu.edu, ckenned2ster@gmail.com, marsteller@pa.msu.edu

We present results from two different procedures for estimation of metallicities ([Fe/H]) and carbon abundance ratios ([C/Fe]) based on a sample of 582 calibration stars of known composition. This sample is much larger that used by Rossi et al. (2005), due to the dramatic increase in the number of stars with elemental abundances measurements obtained from high-resolution analyses in the past few years. This work also compares results obtained from a new calibration on the *KP* and *GP* indices with that obtained from a custom set of spectral synthesis based on MOOG.

10th Symposium on Nuclei in the Cosmos
Mackinac Island, Michigan, USA
27 July – 1 August, 2008

[1] This work is supported, in part, by grants awarded by CNPq, Fapesp, CAPES, and the US National Science Foundation

PoS(NIC X)235

1. Introduction

A large fraction of the most metal-poor stars in the Galaxy, on the order of 20-25%, exhibit strong absorption lines due to the presence of molecular carbon species. Furthermore, it appears [1, 2, 3 (hereafter Paper I)] that the frequency of carbon-enhanced stars ([C/Fe] > +1.0) in the Galaxy increases dramatically at the lowest metal abundances. Over 40% of all stars with [Fe/H] < -3.5 exhibit carbon enhancements, while the fraction rises to 100% (3 of 3) for stars below [Fe/H] = -4.5. The so-called Carbon-Enhanced Metal-Poor (CEMP) stars also exhibit several different patterns of the heavy elements (beyond the iron peak). At least four categories exist, (1) those with s-process-element enhancement (CEMP-s), (2) those with r-process enhancement (CEMP-r), those with both r- and s-process enhancement (CEMP-r/s), and (4) those with no s- or r-process enhancement (CEMP-no). Fully satisfactory explanations for the astrophysical origins of these different classifications are not yet available, although it seems likely that the production of s-process enhancements is associated with mass transfer from an extinct AGB companion in a binary configuration with the presently observed surviving member. It has been suggested that the CEMP-no stars (which tend to occur among stars of the lowest metallicities, [Fe/H] < -2.7 [4]) might have formed from gas that was polluted by the winds from massive, rapidly rotating stars with [Fe/H] < -6.0 [5].

In order to better address the question of the origin of the CEMP phenomenon, large samples of metal-poor stars with available measurements of [C/Fe] and [Fe/H] must be obtained. In the past, this has led to the development of methods for the estimation of these quantities based on medium-resolution (R ~2000) spectra (rather than much more time-intensive high-resolution spectroscopic approaches). However, it has also been recognized that the existing calibration for determination of [C/Fe] and [Fe/H] (Paper I), based on the *KP* (the CaII K line index) and *GP* (the G-band index) indices, is less than ideal near the "edges" of the parameter space, e.g., either at high T_{eff}, low T_{eff}, or when the *GP* index approaches saturation. Here we seek to improve this calibration based on a much larger set of stars with known [C/Fe] and [Fe/H].

2. Data

The sample for this analysis consists of 582 calibration stars with existing determinations of [C/Fe] and [Fe/H] from high-resolution spectroscopy, and with measured CaII K line (*KP*) and CH G band (*GP*) indices from medium-resolution spectroscopy, as well as broadband $(J - K)_0$ colors. Synthetic spectra have also been employed, in order to derive predicted line index and color information based on MARCS and KURUCZ model atmospheres.

3. Analysis

Two different procedures are used to determine estimates of metallicities and carbon abundances – polynomial regression for the calibration sample, and estimation based on

comparison with predicted values from spectrum synthesis and model atmosphere calculations, as discussed below.

3.1 Polynomial Regression

The calibration sample was first divided in two parts, labelled DU and DL, according to the following:

- [log (*GP*) – log (KP)] ≥ – 0.2 → DU: CEMP stars; [C/Fe] > +1.0
- [log (*GP*) – log (KP)] < – 0.2 → DL: NON-CEMP stars; [C/Fe] < +1.0

Figure 1 shows the distribution of *LGP–LKP* for the calibration stars as a function of $(J - K)_0$ color, where *LKP* and *LGP* are the base 10 logarithms of *KP* and *GP*, respectively. The majority of the carbon-rich stars are located above the −0.2 line, although some stars with high carbon abundance fall below this line. We explored a number of different regression models involving second-order terms and cross terms with *LGP* and *LKP*, but the best average residuals were achieved using first-order terms alone. For the purpose of this calibration, objects that exhibited residuals greater than |1σ| were considered outliers and were set aside in the next step, which consists of running the polynomial regression again for the clean sample.

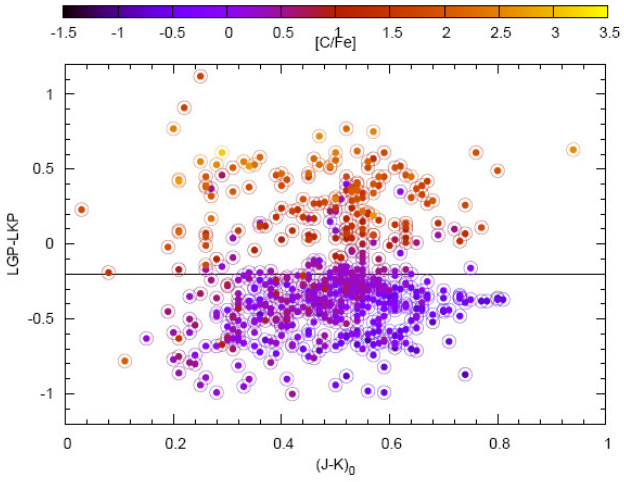

Fig. 1. Behavior of *LKP-LGP* for carbon-enhanced (lighter colors) and non carbon-enhanced stars (darker colors).

The regression relations obtained in Paper I tended to produce [Fe/H] estimates that were too low for stars at the metal-rich end of the calibration. Our new calibration effectively removes this effect once it considers a much larger sub-divided sample of calibration stars. The upper part of the distribution in *LGP–LKP* is the carbon-rich subsample, so a stronger dependence on *GP* is expected. The standard deviation of residuals is 0.246 dex, with a multiple linear correlation coefficient of 0.938. For the lower part of Figure 1, the low-carbon

stars do not have strong GP dependence, so the [Fe/H] estimate depends only on the *KP* index and $(J\text{-}K)_0$ color. In this case, the standard deviation is 0.235 dex, with a multiple linear correlation of 0.919.

Carbon abundances in Paper I were estimated using the relations *without* the split in *LGP*−*LKP*. We could note two distinct behaviors for [C/Fe], justifying the constraints adopted above. There is no dependence of [C/Fe] on $(J-K)_0$ color. Essentially, this means that the variation of KP and GP with T_{eff} is supplying the required temperature information. As a result, there is no need for photometry to determine this quantity. For the carbon-rich part of the diagram in Figure 1, the standard deviation is 0.246 dex, with a multiple linear correlation coefficient of 0.938. For the lower portion of this diagram (low carbon content) , the standard deviation of the residuals is 0.167 dex, with a multiple linear correlation coefficient of 0.868. The residuals for this sample are smaller than those for the carbon-rich sample, due to better determinations of [C/Fe] for lower carbon enhancements.

Our tests confirm that, although estimates of [Fe/H] require $(J\text{-}K)_0$, the determination of [C/Fe] can be produced based on the *KP* and *GP* indices alone.

3.2 Robust and Resistant Polynomial Fits

In order to evaluate the impact of small "local" variations in the parameter space for the synthetic spectra, we decided to apply a local polynomial regression fitting analysis, resistant to the presence of outliers, which produces a lookup table with which one can search for the [Fe/H] and [C/Fe] values based on the line indices and color data. This analysis fits a second-order polynomial surface determined by one or more numerical predictors (*LKP*, *LGP*, and $(J\text{-}K)_0$) using local fitting. In this work, we employ a "span" parameter, which controls the degree of smoothing. The choice of this value is based on the compromise between the influence of distant points and the rapidity with which the local behavior is changing. For example, the lower the span, the better one can reproduce the surface data (which is not uniformly well populated over the calibration surface), and the lower the influence from the rest of the data, but with higher local fluctuations. The 0.5 value indicates that for each point on the grid of model parameters, the nearest 50% of the full grid space is fitted to this function and evaluated at the center of the grid point under consideration. We used a set of model atmospheres including Kurucz and MARCS that have a temperature range of 4000 K to 10000 K. The parameters used to determine [Fe/H] are the *LKP* and the $(J\text{-}K)_0$ color. The parameters used to determine [C/Fe] are *LKP* and *LGP*, as in the regression analysis described above.

In the first step we used a LOESS (a locally weighted robust regression) approach that fits a 2nd order polynomial to the predicted line indices and colors of derived from the models. We then used the surface fit to the models to predict the values of [Fe/H] and [C/Fe] for the set of 582 calibration stars. The next step uses these residuals to correct the original prediction based on the models. To do this, another 2nd order polynomial is fit to the first set of residual values in the same manner described above. This second surface fit provides a correction matrix to the values calculated from the models. Space limitations preclude showing a representation of the [Fe/H] residuals, but Fig. 2 shows the final set of residuals obtained by subtracting the known

values from the corrected calibration predictions for [C/Fe]. The final residuals are substantially improved, and it was possible to remove small remaining correlations between the residuals and the final predictions. Similar improvements were noted for the determination of [Fe/H]. The result of this procedure is the production of a lookup table, whereby the best estimates of [Fe/H] and [C/Fe] based on the input parameters LKP, LGP, and $(J - K)_0$ can be readily accessed by the interested researcher.

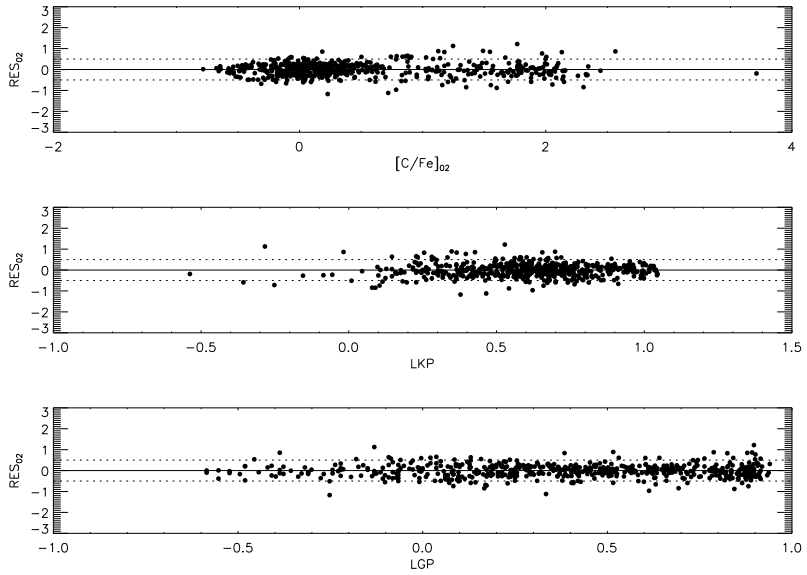

Fig. 2. Residuals for the corrected [C/Fe] based on a robust and resistant local regression analysis. Note that there appears little, if any, dependence on either the derived [C/Fe] (indicating that essentially all of the regression power of the predictors is being fully utilized), or the predictors (in this case LKP and LGP).

References

[1] T. C. Beers & N. Christlieb 2005, *The Discovery and Analysis of Very Metal-Poor Stars in the Galaxy, ARA&A,* **43**, 531

[2] J. E. Norris, S. G. Ryan & T. C. Beers 1997, *Extremely Metal-poor Stars. IV. The Carbon-rich Objects, ApJ,* **488**, 350

[3] S. Rossi, T. C. Beers, C. Sneden, T. Sevastyanenko, J. Rhee, & B. Marsteller 2005, *Estimation of Carbon Abundances in Metal-Poor Stars. I. Application to the 'StrongG-Band' Stars of Beers, Preston, & Shectman, AJ,* **130,** 2804

[4] W. Aoki, T.C. Beers, N. Christlieb, J.E.Norris, S.G. Ryan, & S. Tsangarides 2007, *Carbon-Enhanced Metal –Poor Stars. I. Chemical Compositions of 26 Stars, ApJ,* **655**, 492

[5] G. Meynet, G., S. Ekstrom, A, Maeder, R. Hirschi, C. Chiappini, & C. Georgy 2008, *SPINSTARS at Low Metallicities*, in FIRST STARS III, *AIP Conference Proceedings*, **990**, pp. 212-216